Origin of Rotational Barriers of the N−N Bond in Hydrazine: NBO Analysis

Jong-Won Song,[†] Ho-Jin Lee,[†] Young-Sang Choi,[†] and Chang-Ju Yoon*[,‡]

Department of Chemistry, Korea University, 1 Anam-dong, Seoul 136-701, Korea, and Department of Chemistry, The Catholic University of Korea, Pucheon 420-743, Korea

Received: October 10, 2005; In Final Form: November 20, 2005

Hydrazine passes through two transition states, TS1 ($\phi = 0°$) and TS2 ($\phi = 180°$), in the course of internal rotation around its N−N bond. The origin of the corresponding rotational barriers in hydrazine has been extensively studied by experimental and theoretical methods. Here, we used natural bond orbital (NBO) analysis and energy decomposition of rotational barrier energy ($\Delta E_{barrier}$) to understand the origin of the torsional potential energy profile of this molecule. $\Delta E_{barrier}$ was dissected into structural (ΔE_{struc}), steric exchange (ΔE_{steric}), and hyperconjugative (ΔE_{deloc}) energy contributions. In both transition states, the major barrier-forming contribution is ΔE_{deloc}. The TS2 barrier is lowered by pyramidalization of nitrogen atoms through lowering ΔE_{struc}, not by N−N bond lengthening through lowering ΔE_{steric}. Higher pyramidality of nitrogen atoms of TS2 than that of TS1 explains well why the N−N bond of TS2 is longer than that of TS1. Finally, the steric repulsion between nitrogen lone pairs does not determine the rotational barrier; nuclear−nuclear Coulombic repulsion between outer H/H atoms in TS1 plays an important role in increasing ΔE_{struc}. Taken together, we explain the reason for the different TS1 and TS2 barriers. We show that NBO analysis is a useful tool for understanding structures and potential energy surfaces of compounds containing the N−N bond.

1. Introduction

To understand conformational behaviors of chemical and biochemical compounds that contain the N−N bond, many studies have been performed both experimentally and by theoretical methods.[1−10] Due to its structural simplicity, hydrazine has been extensively studied as a model compound.[2−8] Despite the apparent absence of complicating factors, such as substituents, the origin of the barrier to its internal rotation about the N−N bond seems not to be either simple or fully resolved.

For hydrazine, two transition states (TS1 and TS2) are found during the rotation around the N−N bond[2] (Figure 1 and Table 1). The barrier of GS (ground state) → TS1 is higher than that of GS → TS2.[2] The predominant explanation of rotational barriers about the N−N bond is that the repulsion between nitrogen lone pairs, N(lp)s, determines the barriers and affects the structural changes, such as N−N bond lengthening.[3,10] Several studies, however, suggested that hyperconjugation interactions might determine the barrier.[7] They reported that the barrier to rotation about the N−N bond in hydrazine resulted from the delocalization energy that stabilizes the ground state conformation.[7] Although these studies gave an insight into the origin of the barrier, it did not answer the question of the different TS1 and TS2 barriers in hydrazine and the structural changes during the rotation.

Goodman et al. analyzed rotational barriers ($\Delta E_{barrier}$) of several small model compounds by dissecting them into the structural ($\Delta E_{struct.}$), steric exchange ($\Delta E_{steric.}$) and hyperconjugative ($\Delta E_{deloc.}$) energy contributions.[11,12] They used this method to determine the origin of conformational preference and rotational barriers related to torsions around the C−C or C−O bond of several molecules, including ethane, methanol, dimethyl ether.[11,12] Here, we apply this method to analyze the rotational barrier of hydrazine. We explain the reason the barrier of GS

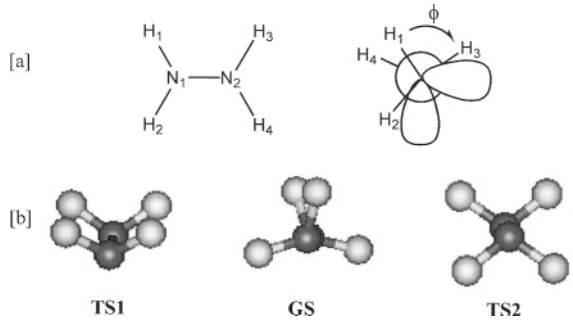

Figure 1. Chemical structure of hydrazine. (a) Atomic numbering of hydrazine and nomenclature. (b) Optimized structures of the ground states (GS) and transition states (TS1 and TS2) at the B3LYP/6-31++G** level of theory.

TABLE 1: Degrees of Hybridization of lp(N), ∑N, Bond Lengths, Bond Angles, and Torsional Angle for TS1, TS2, and GS Geometries in Hydrazine Optimized at the B3LYP/6-31++G Level of Theory**

parameter[a]	TS1	GS	TS2
N1−N2	1.477	1.431	1.483
N1−H1(=N2−H4)	1.019	1.015	1.021
N1−H2(=N2−H3)	1.019	1.019	1.021
∠H1−N1−N2 (=∠N1−N2−H4)	108.8	108.1	104.3
∠H2−N1−N2 (=∠N1−N2−H3)	108.8	113.0	104.3
∠H1−N1−H2 (=∠H3−N2−H4)	105.5	108.8	103.4
∑N	323.1	329.9	312.1
∠H1−N1−N2−H3	0.0	91.2	180.0
s character (%)	26.35	20.72	31.22
p character (%)	73.54	79.19	68.68

[a] Bond lengths in Å; bond angles and dihedral angle in degrees.

* Corresponding author. Tel: 82-2-2164-4330. Fax: 82-2-2164-3764. E-mail: cjyoon@catholic.ac.kr.
[†] Korea University.
[‡] The Catholic University of Korea.

10.1021/jp055755c CCC: $33.50
Published on Web 01/19/2006

→ TS1 (TS1 barrier) is higher than that of GS → TS2 (TS2 barrier) and the origin of structural changes of hydrazine during the rotation.

2. Computational Methods

All calculations were performed at the B3LYP/6-31++G** level using Gaussian 98 software[13] and the NBO 4.0 module.[14] Potential energy surface of the N−N bond rotation was obtained by intrinsic reaction coordinate (IRC) calculations[15] in the transition states (TS1 and TS2). All of the energy barrier calculations were performed without zero-point vibrational correction.

A. Natural Bond Orbital Analysis. NBO (Natural Bond Orbital) analysis[16] is based on a method that transforms wave functions into one center (lone pair) and two center (bond) representations. NBO analysis[16] provides an insight into interactions between various parts of molecules. The diagonal elements of the Fock matrix in the NBO representation represent the energies of localized bonds, lone pairs, and antibonds. Off-diagonal elements represent bond/antibond, lone pair/antibond, and antibond/antibond interactions.

B. Energy Decomposition. It is possible to analyze the barrier using an energy decomposition expressed in terms of the changes in the kinetic and potential energy components.[17] Another way to approach the problem, as taken by Weinhold,[16a,18] partitions the barrier into "Lewis" (ΔE_{lewis}) and delocalization energy changes:

$$\Delta E_{\text{barrier}} = \Delta E_{\text{deloc}} + \Delta E_{\text{lewis}} \tag{1}$$

Lewis energy represents the energy of hypothetical localized species described by a determinant of doubly occupied NBOs comprising the core, lone-pairs, and localized bonds of the Lewis structure. The delocalization energy change, ΔE_{deloc}, represents the hyperconjugative stabilization contribution to the rotational barrier, and in the NBO scheme it arises from bond → antibond charge transfers.[18,19] In the case of ethane, ΔE_{deloc} was found to be the dominant contribution to $\Delta E_{\text{barrier}}$.[11,12]

One objection to the energy decomposition scheme of eq 1 is that it may place too much emphasis on ΔE_{deloc}, because of the composite nature of ΔE_{lewis}, which lumps possibly antagonistic steric and valence effects. Another is that it obliterates separate steric and valence dependencies on relaxation and environmental effects. To provide a more transparent relaxation analysis of the barrier energy, we separate out the steric effect by partitioning ΔE_{lewis} into structural (ΔE_{struc}) and steric exchange (ΔE_{steric}) energy changes.[11,12]

$$\Delta E_{\text{barrier}} = \Delta E_{\text{deloc}} + \Delta E_{\text{steric}} + \Delta E_{\text{struc}} \tag{2}$$

The steric exchange energy change represents the energetic cost to preserve the mutual orthogonality of filled orbitals on atoms that are forced into spatial proximity by the rotation[20b,21] but does not include Coulombic repulsion. Steric exchange repulsions involve a collective response of the entire N-electron system, denoted as "total exchange repulsion" to discriminate this simultaneous all-electron effect from the total pairwise exchange energy obtained by summing independent pair exchange interactions between bond NBOs.[21]

The structural energy change,[11] ΔE_{struc}, represents the energy of the localized species defined by the Lewis structure, but now described by a (nonorthogonalized) preNBO Hartree product. It takes into account Coulombic and bond energy changes in the classical structural formula during internal rotation. Although it retains the stereoelectronic effects associated with the Lewis covalent structure representation, it does not contain the exchange repulsions inherent in ΔE_{lewis} defined through eq 1. It may depend on bond length changes and will be strongly relaxation dependent. We can obtain ΔE_{struc} by calculating the energy change obtained by eliminating the charge-transfer interactions (NOSTAR deletion in NBO 4.0[14]), and the steric repulsion interactions:

$$\Delta E_{\text{NOSTAR}} = \Delta E_{\text{steric}} + \Delta E_{\text{struc}} \tag{3}$$

ΔE_{deloc} can therefore be calculated from full barrier energy defined in eq 2.

C. Bond/Antibond Interactions. The bond/antibond interaction energies[18] provide important information on the interactions between various parts of the molecules. In the case of hydrazine, the energies obtained for the ground and transition states can be used to understand the structures and rotational barriers. The calculations to obtain the bond/antibond interaction energies were executed by the indirect procedure suggested by Wesenberg and Weinhold.[18b] The difference between transition and ground-state energies was calculated with the Fock matrix element, F_{ij^*}, between the bond (or lone pair) NBO φ_i (with an occupancy of nearly 2) and a virtually unoccupied antibond orbital, φ_{j^*} deleted:

$$\Delta E[F^{\text{del}}{}_{ij^*}] = E_{\text{TS}}[F^{\text{del}}{}_{ij^*}] - E_{\text{GS}}[F^{\text{del}}{}_{ij^*}] \tag{4}$$

Here $F^{\text{del}}{}_{ij^*}$ indicates F_{ij^*} deleted. The energy contribution engendered by F_{ij^*} deletion, $\Delta^2 E[F^{\text{del}}{}_{ij^*}]$, is defined as the difference between the barrier energy without deletion, $\Delta E(\text{B}) = E_{\text{TS}} - E_{\text{GS}}$, and the barrier energy calculated form eq 4, $\Delta E[F^{\text{del}}{}_{ij^*}]$

$$\Delta^2 E[F^{\text{del}}{}_{ij^*}] = \Delta E(\text{B}) - \Delta E[F^{\text{del}}{}_{ij^*}] \tag{5}$$

Equation 5 can be rewritten as follows:

$$\Delta^2 E[F^{\text{del}}{}_{ij^*}] = \Delta E_{\text{GS}} - \Delta E_{\text{TS}} \tag{6}$$

Here ΔE_{GS} represents the energy change in the ground state when the corresponding interaction is deleted ($=E_{\text{GS}}[F^{\text{del}}{}_{ij^*}] - E_{\text{GS}}$) and ΔE_{TS} represents the energy change with the corresponding deletion in the transition state ($=E_{\text{TS}}[F^{\text{del}}{}_{ij^*}] - E_{\text{TS}}$). Principal bond/antibond interaction energies for hydrazine are listed in Table 4.

D. Pauli Steric Repulsions. The exchange energy was expressed in terms of the difference between the Hartree-product wave functions for orthogonal and nonorthogonal bond orbitals, which was approximated as the sum of orbital energy changes due to orthogonalization. Specifically, the steric exchange energy,[20,21] if expressed as the sum of energy differences between the filled orthonormal NBOs$\{\bar{\sigma}_I\}$ and their "pre-orthogonal" PNBO counterparts $\{\sigma_I\}$, can be defined as

$$E^{\text{NBO}}{}_{\text{exchange}} = \sum_I (F^{\text{NBO}}{}_{I,I} - F^{\text{PNBO}}{}_{I,I}) \tag{7}$$

Here $F^{\text{NBO}}{}_{I,I} = \langle\bar{\sigma}_I|\hat{F}|\bar{\sigma}_I\rangle$ and $F^{\text{PNBO}}{}_{I,I} = \langle\sigma_I|\hat{F}|\sigma_I\rangle$, $\hat{F}$ being the Fock operator.

The PNBOs differ from the NBOs only in the final interatomic orthogonalization, in which each orbital distorts to include a small oscillatory feature (an "antisymmetrization tail") in regions where it passes through other filled orbitals, raising the energy relative to that of its nonorthogonal counterpart and thereby giving rise to "pressure" as described by Weisskopf.[22] The steric exchange energy is defined as the sum of these energy

changes over all filled orbitals including those (e.g., core orbitals) that are not expected to contribute to the rotational barriers. It was shown that inclusion of all orbitals is necessary for a physically realistic description of steric phenomena, because exchange antisymmetry involves all *J* electrons simultaneously.

ΔE_{steric}, the change of steric exchange repulsion energy between transition and ground state, is

$$\Delta E_{\text{steric}} = E^{\text{NBO}}{}_{\text{exchange}}(\text{TS}) - E^{\text{NBO}}{}_{\text{exchange}}(\text{GS}) \quad (8)$$

2*2 pairwise steric interaction between pairs of orbitals *I* and *J* can be expressed as follows:[20,21]

$$E^{\text{x}}{}_{I,J} = (F^{\text{NBO}}{}_{I,I} - F^{\text{PNBO/2}}{}_{I,I}) + (F^{\text{NBO}}{}_{J,J} - F^{\text{PNBO/2}}{}_{J,J}) \quad (9)$$

Here each "PNBO/2" orbital is formed from "deorthogonalizing" only orbitals *I* and *J* in a reverse Löwdin transformation. The exchange energy can be further approximated as the sum of steric interactions between pairs of orbitals *I* and *J*:

$$E^{2*2}{}_{\text{exchange}} = \sum_{I<J} E^{\text{x}}{}_{I,J} \quad (10)$$

Therefore, the total change of 2*2 pairwise steric exchange repulsion energy between transition and ground state is

$$\Delta E^{2*2}{}_{\text{steric}} = E^{2*2}{}_{\text{exchange}}(\text{TS}) - E^{2*2}{}_{\text{exchange}}(\text{GS}) \quad (11)$$

It has been reported that for interactions of a rare gas atom with another rare gas atom or molecule, this pairwise sum is a relatively good estimate of the full $E^{\text{NBO}}{}_{\text{exchange}}$. For other intermolecular interactions, however, it failed to describe the correct physical behavior of the exchange potential because it does not incorporate the important higher-order coupling effects with other electron pairs.[20,21] Therefore, we used this 2*2 pairwise steric exchange repulsion energy to investigate the steric interactions between lone pairs of N atoms with care.

E. Bond Energies. The bond energy change($\Delta\omega$) is obtained through the following equation:[23]

$$\Delta\omega = \epsilon_{\text{TS}}\rho_{\text{TS}} - \epsilon_{\text{GS}}\rho_{\text{GS}} \quad (12)$$

Here ϵ_{GS} and ϵ_{TS} signify the NBO bond energy of the ground and transition states. The ρ_{GS} and ρ_{TS} indicate the charge occupancy of the corresponding state, respectively. The steric exchange energy is calculated as an energy difference between PNBO's and final NBO's, in terms of diagonal Fock matrix elements. PNBO bond energy was obtained by subtracting steric exchange energy from NBO bond energy.[11,21] ΔE_{struc} represents the energy that accounts for the changes in the highly occupied PNBO orbitals, including, for example, Coulombic interactions, but excluding energy effects due to the charge-transfer and the exchange repulsion. Goodman et al. approximated ΔE_{struc} in the following manner:[11]

$$\Delta E_{\text{struc}} \approx \sum E_{\text{bonds}} \approx \sum \Delta\omega_i \quad (13)$$

Here $\Delta\omega_i$ is the PNBO energy change corresponding to the individual bond (or core) energy change accompanying rotation.

3. Results and Discussion

A. Geometries and Rotational Barriers of Hydrazine. The GS conformation has a dihedral ϕ angle of 91.2° (Figure 1). TS1 and TS2 conformations have ϕ angles of 0° and 180°, respectively. The dihedral ϕ angle of H1−N1−N2−H3 is the same as the dihedral angle of lp-N−N-lp [lp(N) = lone pair of N atom]. Figure 2 is the rotational profile as a function of ϕ dihedral angle in hydrazine, obtained by an IRC calculation[15] from TS1 and TS2 at the B3LYP/6-31++G** level of theory. During rotation about the N−N bond, the structural changes also occurred.[4] The N−N bond length in GS, TS1, and TS2 conformations is 1.431, 1.477, and 1.483 Å, respectively (Table 1). It is interesting to note that the N−N bond of TS2 is slightly longer than that of TS1.[2,4,10] In addition, the sum of three angles around the N atom, denoted by ∑N, is decreased during the rotation. The ∑N of GS, TS1, and TS2 conformations is 329.9°, 323.1°, and 312.1°, respectively. This shows that the N atom of TS2 is more pyramidalized than that of TS1. Because pyramidalization of N atoms is related to rehybridization of lp(N)s, the degree of hybridization of lp(N)s in GS, TS1, and TS2 conformations is $sp^{3.82}$, $sp^{2.79}$ and $sp^{2.20}$, respectively, by NBO analysis[16] at the B3LYP/6-31++G** level of theory. This shows that when pyramidality of N atoms increases, the p character (%p) of lp(N)s decreases, which may result in an increase of %p of N−N bond. The TS1 barrier is predicted to be 9.99 kcal/mol and the TS2 barrier is 3.05 kcal/mol (Table 2). The TS1 barrier is about 3 times higher than the TS2 barrier.[2] Therefore, only the TS2 barrier has been observed experimentally.[6]

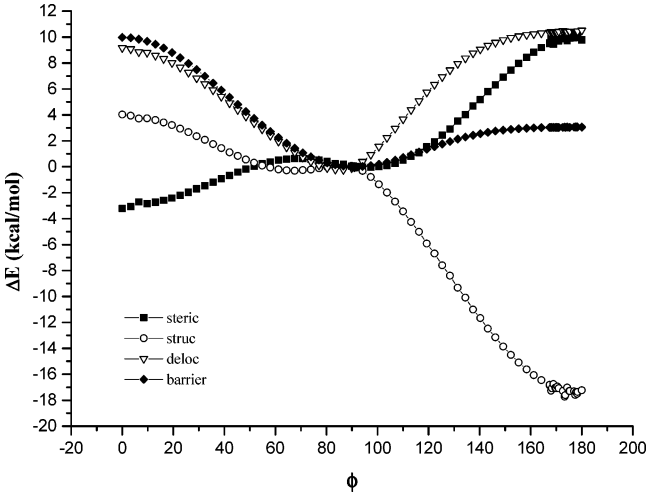

Figure 2. Rotational dependence of the energy components and barrier energies of fully relaxed rotation leading to TS1 and TS2, obtained by IRC calculations at the B3LYP/6-31++G** level of theory.

TABLE 2: Change of Rotational Energy Barrier (kcal/mol), ∑N (deg), N−H Bond Length (Å), and N−N Bond Length (Å) According to Rigid, Partially Relaxed, and Fully Relaxed Rotation in TS1 and TS2 of Hydrazine[a]

	N−N relaxed	X−N−X relaxed	N−H relaxed	rigid	fully relaxed
			TS1 ($\phi = 0°$)		
$\Delta E_{\text{barrier}}$	11.04	10.61	11.46	11.47	9.98
N−N	1.464	1.431	1.431	1.431	1.477
N1−H1	1.0148	1.0148	1.0167	1.0148	1.01925
N1−H2	1.0186	1.0186	1.0160	1.0186	1.01925
∑N	329.9	325.7	329.9	329.9	323.1
			TS2 ($\phi = 180°$)		
$\Delta E_{\text{barrier}}$	6.81	3.87	6.90	6.92	3.06
N−N	1.448	1.431	1.431	1.431	1.483
N1−H1	1.0148	1.0148	1.0142	1.0148	1.02065
N1−H2	1.0186	1.0186	1.0140	1.0186	1.02065
∑N	329.9	315.0	329.9	329.9	312.1

[a] All calculations were performed at the B3LYP/6-31++G** level of theory.

B. Skeletal Relaxation. During the rotation of the N−N bond, hydrazine undergoes structural changes. In other words, N−N bond lengthening, N−H bonds lengthening, and pyramidalization of N atom occur simultaneously during the rotation.[2,4,10] To understand the effect of structural changes on the barrier, we rigidly rotated N−N bond, and then geometrically optimized the selected one component from the pool of the N−N bond, all the N−H bonds, or all the X−N−X angles.[23]

In Table 2, $\Delta E_{\text{barrier}}$'s of N−H bond relaxed rotation of both TS1 and TS2 (TS1, 11.46 kcal/mol; TS2, 6.90 kcal/mol) are almost the same as those of rigid rotation (11.47 kcal/mol; 6.92 kcal/mol). Moreover, N−H bonds lengthen by at most 0.0046 Å in N−H bond relaxed rotation, implying that the effect of N−H bonds lengthening on the barrier energy can be neglected.

In TS1, $\Delta E_{\text{barrier}}$ of X−N−X angle relaxed rotation (10.61 kcal/mol) is similar to that of fully relaxed rotation (9.98 kcal/mol), whereas $\Delta E_{\text{barrier}}$ of the N−N bond relaxed rotation (11.04 kcal/mol) is close to that of rigid rotation (11.47 kcal/mol). This shows that pyramidalization of N atoms lowers rotational barrier more effectively in TS1 than N−N lengthening does.

In TS2, $\Delta E_{\text{barrier}}$ of X−N−X angle relaxed rotation (3.87 kcal/mol) is similar to that of fully relaxed rotation (3.06 kcal/mol), whereas $\Delta E_{\text{barrier}}$ of N−N bond relaxed rotation (6.81 kcal/mol) is almost equal to $\Delta E_{\text{barrier}}$ of rigid rotation (6.92 kcal/mol). This shows that, in case of TS2, pyramialization is more important than N−N bond relaxation in lowering $\Delta E_{\text{barrier}}$. Compared with the fully relaxed rotation (1.483 Å), the N−N bond length of N−N bond relaxed rotation (1.448 Å) is not lengthened so much and is close to that of rigid rotation (1.431 Å). It seems that pyramidalization of N atoms in the transition states plays a crucial role in lowering $\Delta E_{\text{barrier}}$, compared with N−N bond lengthening, which has been known as the principal barrier lowering mechanism.[10] As pyramidality of the N atoms increases, the %p of lp(N)s decreases, which results in increasing of the %p of N−N bond. We reasoned that the increasing of pyramidality of N atoms in TS2 results in N−N bond lengthening in TS2.

C. Decomposition of Rotational Barrier. To evaluate the nature of the barrier to rotation about the N−N bond, we decomposed the rotational barrier into three different contributions, ΔE_{struc}, ΔE_{steric}, and ΔE_{deloc} (Table 2 and Figure 2). For the TS1 barrier, the contributors ΔE_{deloc} and ΔE_{struc} are barrier forming, whereas the term ΔE_{steric} lowers the barrier. For TS2 barrier, ΔE_{deloc} and ΔE_{steric} are the barrier-forming contributors, whereas ΔE_{struc} is the important anti-barrier-forming contributor.

In rigid rotation model, ΔE_{deloc} is the barrier-forming contributor in both transition states (Figure 3). In the course of rigid rotation leading to TS1, ΔE_{steric} and ΔE_{struc} also contribute to an increase in barrier energy (2.42 and 2.98 kcal/mol, respectively), which is the reason for $\Delta E_{\text{barrier}}$ of rigid rotation in TS1 (11.47 kcal/mol) being higher by 4.55 kcal/mol than that in TS2 (6.92 kcal/mol). On the other hand, ΔE_{steric} and ΔE_{struc} of rigid rotation are almost zero (+0.51 and −0.49 kcal/mol, respectively) in TS2. Nevertheless, in fully relaxed rotation they are split to be largely positive and negative values, respectively (Figure 2). In both rigid and fully relaxed rotation, ΔE_{deloc} is the important barrier-forming contributor for barrier (Table 2). The energy decomposition scheme implies that the different barrier heights in hydrazine result from the different contribution of ΔE_{struc} and ΔE_{steric} terms, which are related with N−N bond lengthening and pyramidalization of N atoms. We thus investigated the effect of structural changes on the barrier energy by using the internal rotational paths[11] (Figure 4 and Table 3). Path A rotates the torsional dihedral angle in the GS structure to its value in TS1 or TS2, freezing all the other angles and bond lengths (step I). This is followed by relaxing $-NH_2$ internal angles to their fully relaxed values (step II). This is followed by N−N bond relaxation (step III). Finally, step VI relaxes all of the N−H bonds to their fully relaxed values. Path B rotates the torsional dihedral angle in the GS structure as step I. This is followed by N−N bond relaxation (step IV), then by relaxing $-NH_2$ internal angles to their fully relaxed values (step V), and finally by step VI, which relaxes all of the N−H bonds to the fully relaxed values.

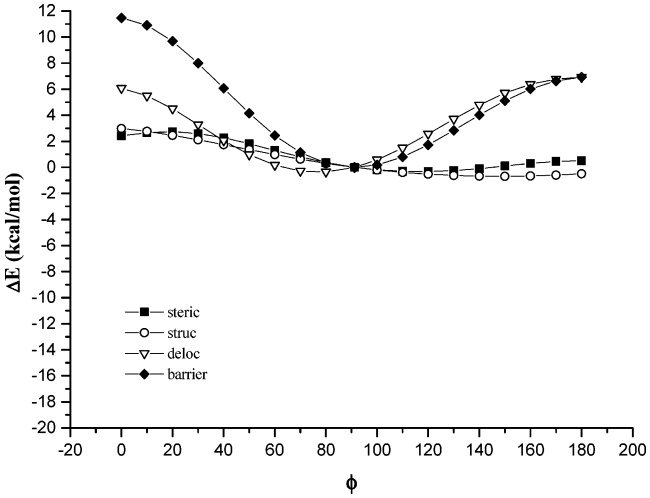

Figure 3. Rotational dependence of energy components and barrier energies of rigid rotation leading to TS1 and TS2, calculated at the B3LYP/6-31++G** level of theory.

Table 3 shows that N−N bond relaxation and pyramidalization of N atoms are related to lowering $\Delta E_{\text{barrier}}$ and that N−H bond relaxation hardly affects the energy decomposition terms and $\Delta E_{\text{barrier}}$. We summarize Table 3 in the following manner: (1) During the fully relaxed rotation, the increase of ΔE_{deloc} is mainly due to the pure rotation (step I). The N−N bond relaxation also contributes to increasing ΔE_{deloc}. (2) During fully relaxed rotation, N−N bond relaxation makes ΔE_{steric} decrease and ΔE_{struc} increase (steps III or IV). (3) During the fully relaxed rotation, pyramidalization of N atoms makes ΔE_{steric} increase and ΔE_{struc} decrease (steps II and V). (4) In TS2, the most important structural change to lower $\Delta E_{\text{barrier}}$ is pyramidalization of N atoms (see $\Delta E_{\text{barrier}}$, 0.33 kcal/mol, in step IV, path B). This shows clearly that pyramidalization of N atoms is the most important anti-barrier structural change during the fully relaxed rotation in both TS1 and TS2. Because these structural changes affect the rotational barrier energy, we investigated both structural and steric energies in **E** and **F** sections in more detail.

D. Delocalization Energy. The delocalization energy (ΔE_{deloc}) is the most important barrier-forming term of all the energy decomposition terms in both transition states. The most important barrier-forming interactions are N1(lp)/N2−H4(σ*) and N2(lp)/N1−H1(σ*) which amount to 4.26 kcal/mol in GS → TS1 and 5.30 kcal/mol in GS → TS2 (Table 4). These interactions are the principal origin of rotational barriers of hydrazine as shown by Weinhold.[7b] As these interactions have already been analyzed,[7b] we did not discuss them further.

E. Steric Exchange Energy. To understand the role of the local bond orbitals on the barrier, we used the 2*2 pairwise exchange energy that gives the independent pair interactions between local bond orbitals; however, the sum of 2*2 pairwise exchange energies is not the same as ΔE_{steric} and the total 2*2 exchange energy is less accurate than the total steric exchange energy as reported earlier.[20,21] Table 5 shows that the steric

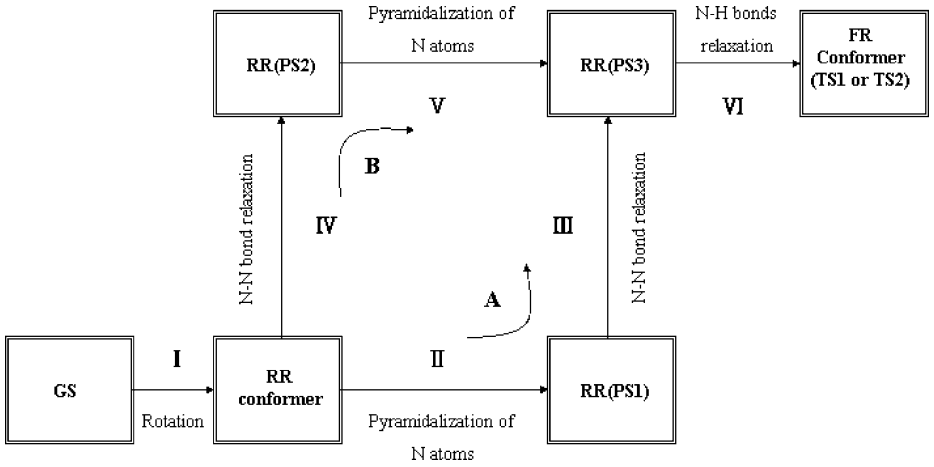

Figure 4. Alternate internal rotation paths to the fully relaxed (FR) hydrazine conformer. In path A: step I, rigid rotation form the GS conformer is followed by relaxation along pyramidalization of N atoms to its optimized TS conformer [the "prepared" conformer state 1, PS1] (step II) and is followed by N−N bond relaxation (step III). In path B: step I, rigid rotation from the GS conformer is followed by relaxation along N−N bond relaxation to its optimized TS conformer to its optimized TS conformer value [the "prepared" conformer state 2, PS2] (step IV) and is followed by pyramidalization of N atoms from PS2 (step V). Step VI relaxes N−H bonds to its fully relaxed value.

TABLE 3: Energy Decomposition of the Rotational Barrier as a Function of Internal Paths[a]

GS → TS1		ΔE_{struc}	ΔE_{steric}	ΔE_{deloc}	$\Delta E_{barrier}$
fully relaxed		4.04	−3.22	9.17	9.98
A	step I	2.98	2.42	6.07	11.47
	step II	−10.43	9.37	0.35	−0.70
	step III	11.09	−14.66	2.81	−0.76
	step VI	0.39	−0.35	−0.06	−0.02
B	step I	2.98	2.42	6.07	11.47
	step IV	11.48	−14.61	2.76	−0.37
	step V	−10.82	9.32	0.40	−1.10
	step VI	0.39	−0.35	−0.06	−0.02
GS → TS2		ΔE_{struc}	ΔE_{steric}	ΔE_{deloc}	$\Delta E_{barrier}$
fully relaxed		−17.22	9.78	10.50	3.06
A	step I	−0.49	0.51	6.91	6.92
	step II	−29.83	27.69	−0.72	−2.86
	step III	12.55	−17.85	4.34	−0.96
	step VI	0.56	−0.57	−0.02	−0.03
B	step I	−0.49	0.51	6.91	6.92
	step IV	13.37	−16.88	3.83	0.33
	step V	−30.66	26.72	−0.21	−4.15
	step VI	0.56	−0.57	−0.02	−0.03

[a] See Figure 4. All calculations were performed at the B3LYP/6-31++G** level of theory.

repulsion between nitrogen lone pairs is higher in TS2 (12.14 kcal/mol) than in TS1 (10.14 kcal/mol)[8,9] and that N−N bond lengthening lowers the steric repulsion between lone pairs. Nevertheless, the 2*2 pairwise steric exchange energy between lone pairs of rigid rotation (RR) in TS1 is lower (13.18 kcal/mol) than that in TS2 (18.33 kcal/mol), whereas ΔE_{steric} of rigid rotation in TS1 is higher (2.42 kcal/mol) than that in TS2 (0.51 kcal/mol). This shows that the steric repulsion between two lone pairs does not dominate the entire steric repulsion during the internal rotation. In addition, the 2*2 pairwise steric exchange energy between lone pairs is decreased by pyramidalization of N atoms (RR → PS1 conformer) in both TS1 and TS2. ΔE_{steric} and the total 2*2 exchange energy, however, are increased by pyramidalization of N atoms in both transition states. In other words, pyramidalization lowers the steric repulsion between lone pairs but heightens ΔE_{steric}. This implies that pyramidalization of N atoms is not related to escaping the repulsion between N(lp)s. The assumption that the origin of rotational barrier of hydrazine is the repulsion between N(lp)s needs to be reconsidered especially in TS2.[10]

TABLE 4: Bond/Antibond Interactions (kcal/mol) of Hydrazine[a]

donor/acceptor interaction	GS → TS1	GS → TS2
Barrier Forming		
N1(lp)/N2−H3(σ*)	0.95	1.99
N1(lp)/N2−H4(σ*)	4.26	5.30
N2(lp)/N1−H2(σ*)	0.95	1.99
N2(lp)/N1−H1(σ*)	4.26	5.30
N1−H1(σ)/N2−H3(σ*)	0.90	1.72
N2−H3(σ)/N1−H2(σ*)	0.90	1.72
Antibarrier Forming		
N1−H1(σ)/N2−H4(σ*)	−0.82	
N2−H4(σ)/N1−H1(σ*)	−0.82	
N1−H2(σ)/N2−H4(σ*)		−1.76
N1−H1(σ)/N2−H3(σ*)		−1.87
N2−H3(σ)/N1−H1(σ*)		−1.76
N2−H2(σ)/N1−H2(σ*)		−1.87
total sum	9.83	11.24
ΔE_{deloc}[b]	9.17	10.50

[a] All calculations were performed at the B3LYP/6-31++G**-optimized geometries. [b] These values were obtained by NOSTAR procedure of NBO4.0.

TABLE 5: 2*2 Pairwise Steric Exchange Energy Changes (kcal/mol) in Hydrazine[a]

TS1	GS	RR	PS1	PS2	FR
LP(N1)/LP(N2)	0.00	13.18	11.16	11.89	10.14
total $E^{2*2}_{exchange}$[b]	36.79	40.56	41.12	34.37	34.81
ΔE^{2*2}_{steric}[c]	0.00	3.77	4.33	−2.42	−1.98
ΔE_{steric}	0.00	2.42	9.37	−14.61	−3.22
TS2	GS	RR	PS1	PS2	FR
LP(N1)/LP(N2)	0.00	18.33	15.29	14.86	12.14
total $E^{2*2}_{exchange}$[b]	36.79	39.45	40.67	32.68	33.80
ΔE^{2*2}_{steric}[c]	0.00	2.66	3.88	−4.11	−2.99
ΔE_{steric}	0.00	0.51	27.69	−16.88	9.78

[a] All calculations were performed at the B3LYP/6-31++G** level of theory. [b] These values were obtained by eq 10. [c] These values were obtained by eq 11.

F. Structural Energy. Structural energy may be represented by PNBO bond energy changes[11] (Table 6). The N−N bond lengthening (steps III and IV) and pyramidalization of N atoms (steps II and V) affect the PNBO energy changes significantly, as compared with other bond or core components. The N−N bond lengthening increases the N−N PNBO energy similarly in both transition states. Nevertheless, pyramidalization of N

TABLE 6: PNBO Bond Energies (kcal/mol) as a Function of Internal Paths[a]

TS1	N1−H2(σ)	N1−H1(σ)	N1−N2(σ)	N1(lp)	N1(core)	$\sum\Delta\omega_i$	ΔE_{struc}
fully relaxed	−9.58	−0.92	48.64	−20.53	−5.69	−24.82	4.04
step I	−9.41	−5.30	−4.05	3.00	1.39	−24.67	2.98
step II	−2.42	4.96	−0.03	−18.32	−0.14	−31.88	−10.43
step III	−0.97	−0.94	53.14	−4.49	−6.07	28.20	11.10
step VI	3.21	0.36	−0.42	−0.72	−0.88	3.52	0.39
step I	−9.41	−5.30	−4.05	3.00	1.39	−24.67	2.98
step IV	−1.31	−0.92	52.32	−3.63	−6.06	28.48	11.48
step V	−2.08	4.94	0.79	−19.18	−0.15	−32.16	−10.81
step VI	3.21	0.36	−0.42	−0.72	−0.88	3.52	0.39
TS2	N1−H2(σ)	N1−H1(σ)	N1−N2(σ)	N1(lp)	N1(core)	$\sum\Delta\omega_i$	ΔE_{struc}
fully relaxed	1.53	10.19	65.09	−56.48	−3.68	−31.78	−17.22
step I	−2.72	4.02	0.31	−1.07	4.50	9.80	−0.49
step II	3.24	8.05	4.50	−48.83	2.46	−65.70	−29.83
step III	−3.23	−3.19	61.09	−5.33	−9.10	19.42	12.54
step VI	4.23	1.31	−0.82	−1.25	−1.55	4.70	0.56
step I	−2.72	4.02	0.31	−1.07	4.50	9.80	−0.49
step IV	−2.62	−2.29	58.86	−2.36	−6.94	30.44	13.37
step V	2.63	7.15	6.73	−51.80	0.30	−76.72	−30.66
step VI	4.23	1.31	−0.82	−1.25	−1.55	4.70	0.5Y

[a] See Figure 4. All calculations were performed at the B3LYP/6-31++G of theory.

TABLE 7: Changes in the Sum of PNBO Bond Energies ($\sum\Delta\omega_i$), Structural Energy (ΔE_{Struc}), and Coulombic Energies (kcal/mol) of Hydrazine[a]

energy change	RR(TS1)	RR(TS2)	TS1	TS1″	TS2
$\sum\Delta\omega_i$	−24.67	9.80	−24.82	−69.64	−31.78
ΔE_{struc}	2.98	−0.49	4.04	−10.53	−17.22
ΔV_{nn}	27.88	−11.83	−384.66	−291.39	−360.10
ΔV_{ee}	3.53	2.27	−400.66	−337.68	−350.61
ΔV_r (=ΔV_{nn} + ΔV_{ee})	31.41	−9.56	−785.31	−629.07	−710.71
ΔV_a (=ΔV_{ne})	−48.09	12.25	796.71	605.04	704.57

[a] All calculations were performed at the B3LYP/6-31++G** level of theory.

atoms affects the N(lp) PNBO energies differently in TS1 and TS2. The decrease of N(lp)s PNBO energies for TS2 is larger than that for TS1 (steps II and V for TS1 and TS2) because of the different pyramidality of N atoms between TS1 and TS2. The decrease of N(lp) PNBO energies significantly contributes to decreasing $\sum\Delta\omega_i$ and ΔE_{struc} (steps II and V for TS1 and TS2), which may explain why the rotational barrier of TS1 is higher than that of TS2.

G. Coulombic Repulsion. Coulombic repulsion energy is another factor that can affect ΔE_{struc}.[11] Coulombic repulsion energy (V_r) consists of electron−electron Coulombic repulsion energy (V_{ee}) and nuclear−nuclear Coulombic repulsion energy (V_{nn}). Coulombic attraction energy (V_a) is the same as nuclear-electron Coulombic attraction energy (V_{ne}), which is related to bond energies and delocalization energy.

As shown in the step I of RR(TS1) and RR(TS2) of Table 7, the relationship between $\sum\Delta\omega_i$ and ΔE_{struc} digresses from eq 5. We therefore investigated Coulombic repulsion energy terms (V_r), in an attempt to explain the reason for the difference between the TS1 and TS2 barriers. ΔV_r of RR(TS1) is positive (31.41 kcal/mol), but that of RR(TS2) is negative (−9.56 kcal/mol). At this point, ΔV_{ee} of ΔV_r in RR(TS1) is almost the same as that in RR(TS2), whereas ΔV_{nn} in RR(TS2) is negative value (−11.83 kcal/mol) and ΔV_{nn} in RR(TS1) is positive value (27.88 kcal/mol). Higher ΔV_{nn} of RR(TS1) than that of RR(TS2) is responsible for the difference of ΔV_r between TS1 and TS2. It seems that ΔE_{struc} of rigid rotation in TS1 (2.98 kcal/mol), which is higher than that in TS2 (−0.49 kcal/mol), results from the difference of ΔV_{nn} between TS1 and TS2. Because there are no nuclei except the nuclei of outer H/H atoms that become closer to each other in case of RR(TS2) → RR(TS1), this implies that ΔV_{nn} between outer H/H atoms makes ΔE_{struc} of rigid rotation in TS1 higher than that in TS2.[4] In addition, the increase of the nuclear−nuclear Coulombic repulsion energy between outer H/H atoms in rigid rotation is the reason that $\Delta E_{barrier}$ in RR(TS1) is higher than in RR(TS2).

TABLE 8: Changes in Rotational Barrier ($\Delta E_{Barrier}$) and Barrier Energy Decomposition Terms (kcal/mol) in TS2, TS1″, and TS1 at the B3LYP/6-31++G and MP2/6-31++G** Levels of Theory**

	ΔE_{struc}	ΔE_{steric}	ΔE_{deloc}	$\Delta E_{barrier}$	exp $\Delta E_{barrier}$[a]
			B3LYP/6-31++G**		
GS → TS1	4.04	−3.22	9.17	9.99	
GS → TS1″	−10.53	10.71	11.70	11.88	
GS → TS2	−17.23	9.78	10.50	3.05	3.145
			MP2/6-31++G**		
GS → TS1	6.55	−5.50	9.16	10.21	
GS → TS1″	−9.24	9.5	11.80	12.06	
GS → TS2	−16.54	9.55	10.00	3.02	

[a] Reference 3.

When N−N bond is rigidly rotated from TS2 to TS1 (TS1″ conformer), $\Delta E_{barrier}$ is increased from 3.05 to 11.88 kcal/mol (Table 8). ΔE_{struc} is enlarged by 6.70 kcal/mol, whereas the other decomposition terms are almost unchanged (≤1.2 kcal/mol). The tendency of these changes of barrier energy and energy decomposition terms are not different from that calculated at the MP2/6-31++G** level of theory. On the other hand, $\sum\Delta\omega_i$ largely increases, whereas ΔV_{nn} increases by 68.71 kcal/mol and ΔV_{ee} increases only by 12.93 kcal/mol. Comparing the change of ΔV_{ee} with that of ΔV_{nn} in TS2 → TS1″, we noted that most of the increase of ΔE_{struc} results from the increase of ΔV_{nn}. We reasoned that the nuclear−nuclear Coulombic repulsion energy between outer H/H atoms makes ΔE_{struc} of rigid rotation in TS1 higher than that in TS2.[4]

4. Conclusions

We analyzed the rotational barrier of the N−N bond in hydrazine using NBO analysis and energy decomposition scheme, such as the structural (ΔE_{struc}), steric exchange (ΔE_{steric}), and hyperconjugative (ΔE_{deloc}) energy contributions. The most important barrier-forming contribution is the delocalization energy (ΔE_{deloc}) at TS1 and TS2 barriers. It is notable that the

difference between the TS1 and TS2 barriers in hydrazine about the N−N bond may be explained by the different pyramidalization of N atoms between TS1 and TS2, which lowers ΔE_{struc} differently. The structural energy of TS1 is much higher than that of TS2, which results from the nuclear−nuclear Coulombic repulsion between outer H/H atoms in TS1. This NBO analysis, therefore, may be helpful in understanding the conformational behavior of compounds that contain the N−N bond[1].

Acknowledgment. We thank V. Pophristic for helpful discussions. C.-J.Y. is obliged to the 2002 Research Fund of the Catholic University of Korea.

References and Notes

(1) (a) Lee, H.-J.; Ahn, I.-A.; Ro, S.; Choi, K.-H.; Choi, Y.-S.; Lee, K.-B. *J. Peptide Res.* **2000**, *56*, 35. (b) Lee, H.-J.; Song, J.-W.; Choi, Y.-S.; Ro, S.; Yoon, C.-J. *Phys. Chem. Chem. Phys.* **2001**, *3*, 1693. (c) Lee, H.-J.; Song, J.-W.; Choi, Y.-S.; Park, H.-M.; Lee, K.-B. *J. Am. Chem. Soc.* **2002**, *124*, 11881. (d) Lee, H.-J.; Jung, H. J.; Kim, J. H.; Choi, Y.-S.; Park, H.-M.; Lee, K.-B. *Chem. Phys.* **2003**, *294*, 201. (e) Lee, H.-J.; Lee, M.-H.; Choi, Y.-S.; Park, H.-M.; Lee, K.-B. *J. Mol. Struct. (THEOCHEM)* **2003**, *631*, 101. (f) Zhang; Wei-Jun; Berglund, A.; Kao, J. L.-F.; Couty, J.-P.; Gershengorn, M. C.; Marshall, G. R. *J. Am. Chem. Soc.* **2003**, *125*, 1221. (g) Lee, H.-J.; Kim, J. H.; Jung, H. J.; Kim, K.-Y.; Kim, E.-J.; Choi, Y.-S.; Yoon, C.-J. *J. Comput. Chem.* **2004**, *25*, 169. (h) Che, Y.; Marshall, G. R. *J. Org. Chem.* **2005**, *69*, 9030.

(2) (a) Chung-Phillips, A.; Jebber, K. A. *J. Chem. Phys.* **1995**, *102*, 7080. (b) Thormann, M.; Hofmann, H.-J. *J. Mol. Struct.* **1999**, *469*, 63.

(3) Smits, G. F.; Krol, M. C.; Altona, C. *Mol. Phys.* **1988**, *63*, 921.

(4) Mastryukov, V. S.; Boggs, J. E.; Samdal, S. *J. Mol. Struct.* **1993**, *288*, 225.

(5) Kohata, K.; Rukuyama, T.; Kusitsu, K. *J. Phys. Chem.* **1982**, *86*, 602.

(6) Kasuya, T.; Kojima, T. *J. Phys. Soc. Jpn.* **1963**, *18*, 364.

(7) (a) Radom, L.; Hehre, W. J.; Pople, J. A. *J. Am. Chem. Soc.* **1972**, *94*, 2371. (b) Brunck, T.; Weinhold, F. *J. Am. Chem. Soc.* **1979**, *101*, 1700.

(8) Habas, M.-P.; Baraille, I.; Larrieu, C.; Chaillet, M. *Chem. Phys.* **1997**, *219*, 63.

(9) Nelsen, S. F.; Buschek, J. M. *J. Am. Chem. Soc.* **1973**, *95*, 2011.

(10) Ma, B.; Lii, J.; Chen, K.; Allinger, N. L. *J. Phys. Chem.* **1996**, *100*, 11297.

(11) (a) Goodman, L.; Gu, H.; Pophristic, V. *J. Chem. Phys.* **1999**, *110*, 4268. (b) Goodman, L.; Pophristic, V. *Acc. Chem. Res.* **1999**, *32*, 983.

(12) (a) Goodman, L.; Pophristic, V. *Nature* **2001**, *411*, 563. (b) Pophristic, V.; Goodman, L. *J. Phys. Chem.* **2002**, *106*, 1642. (c) Pophristic, V.; Goodman, L.; Wu, C. T. *J. Phys. Chem.* **2001**, *105*, 7454. (d) Goodman, L.; Pophristic, V.; Wang, W. *Int. J. Quantum Chem.* **2002**, *90*, 657.

(13) Frisch, M. J.; Trucks, G. W.; Schlegel, H. B.; Scuseria, G. E.; Robb, M. A.; Cheeseman, J. R.; Zakrzewski, V. G.; Montgomery, J. A., Jr.; Stratmann, R. E.; Burant, J. C.; Dapprich, S.; Millam, J. M.; Daniels, A. D.; Kudin, K. N.; Strain, M. C.; Farkas, O.; Tomasi, J.; Barone, V.; Cossi, M.; Cammi, R.; Mennucci, B.; Pomelli, C.; Adamo, C.; Clifford, S.; Ochterski, J.; Petersson, G. A.; Ayala, P. Y.; Cui, Q.; Morokuma, K.; Malick, D. K.; Rabuck, A. D.; Raghavachari, K.; Foresman, J. B.; Cioslowski, J.; Ortiz, J. V.; Baboul, A. G.; Stefanov, B. B.; Liu, G.; Liashenko, A.; Piskorz, P.; Komaromi, I.; Gomperts, R.; Martin, R. L.; Fox, D. J.; Keith, T.; Al-Laham, M. A.; Peng, C. Y.; Nanayakkara, A.; Challacombe, M.; Gill, P. M. W.; Johnson, B.; Chen, W.; Wong, M. W.; Andres, J. L.; Gonzalez, C.; Head-Gordon, M.; Replogle, E. S.; Pople, J. A. *Gaussian 98*, revision A.7; Gaussian, Inc.: Pittsburgh, PA, 1998.

(14) Glendening, E. D.; Badenhoop, J. K.; Reed, A. E.; Carpenter, J. E.; Weinhold, F. *NBO 4.0*; Theoretical Chemistry Institute, University of Wisconsin: Madison, 1996.

(15) (a) Gonzalez, C.; Schlegel, H. B. *J. Chem. Phys.* **1989**, *90*, 2154. (b) Gonzalez, C.; Schlegel, H. B. *J. Phys. Chem.* **1990**, *94*, 5523.

(16) (a) Foster, J. P.; Weinhold, F. *J. Am. Chem. Soc*. **1980**, *102*, 7211. (b) Reed, A. E.; Weinhold, F. *J. Chem. Phys*. **1983**, *78*, 4066. (c) Reed, A. E.; Weinstock, R. B.; Weinhold, F. *J. Chem. Phys*. **1985**, *83*, 735. (d) Reed, A. E.; Weinhold, F. *J. Chem. Phys.* **1985**, *83*, 1736.

(17) Goodman, L.; Kundu, T.; Leszczynski, J. *J. Phys. Chem*. **1996**, *100*, 2770.

(18) (a) Tyrrell, J.; Weinstock, R. B.; Weinhold, F. *Int. J. Quantum Chem*. **1981**, *19*, 781. (b) Wesenberg, G.; Weinhold, F. *Int. J. Quantum Chem*. **1982**, *21*, 487.

(19) Reed, A. E.; Weinhold, F. *Isr. J. Chem*. **1991**, *31*, 277.

(20) (a) Badenhoop, J. K.; Weinhold, F. *J. Chem. Phys.* **1997**, *107*, 5406. (b) Badenhoop, J. K.; Weinhold, F. *J. Chem. Phys.* **1997**, *107*, 5422.

(21) Badenhoop, J. K.; Weinhold, F. *Int. J. Quantum Chem.* **1999**, *72*, 269.

(22) Weisskopf, V. F. *Science* **1975**, *187*, 605.

(23) (a) Goodman, L.; Pophristic, V. *Chem. Phys. Letter*. **1996**, *259*, 287. (b) Kim, W.; Lee, H.-J.; Choi, Y.-S.; Choi, J.-H.; Yoon, C.-J. *Faraday Trans.* **1998**, *94*, 2663.